Contributed paper

OPTO-ELECTRONICS REVIEW 9(4), 413–417 (2001)

Fibre optic distributed sensor of vibration in unbalanced Michelson's interferometer configuration

M. SZUSTAKOWSKI[1], M. CHOJNACKI[2*], M. ŻYCZKOWSKI[1], and N. PAŁKA[1]

[1]Institute of Optoelectronics, Military University of Technology
2 Kaliskiego Str., 00-908 Warsaw, Poland
[2]Institute of Fundamental Electronics – Electronic Department, Military University of Technology
2 Kaliskiego Str., 00-908 Warsaw, Poland

The subject of this work is a novel fibre optic distributed sensor system. The system uses a technique called multiplexed reflectometric interferometry to measure dynamic strain in a network of single mode optical fibre sensors. The sensor is constructed on an unbalanced fibre optic Michelson's interferometer. This article presents influence of the wavelength change of radiation source on the course of interference contrast function of the unbalanced Michelson's interferometer. A digital demodulation with application of a fibre optic coupler 3×3 is also presented. The maximum number of individual sensors is currently limited by the optical power budget and will increase with new technology implementation. The system can address a variety of sensor types for different physical parameters.

Keywords: distributed fibre sensor, unbalanced Michelson's interferometer, sensor of vibration.

1. Introduction

Interferometer as a classical technique is known for over 100 years. First investigations in this discipline were conducted by Michelson in 1881, Mach and Zehnder in 1891, and next by Fabry and Perot in 1899. Fibre-optic interferometer has been developing for the last ten years as a separate type of fibre-optic sensors. Optical configurations of interferometers have been adapted from classical interferometers where the light is lead in optical wave duct. In the scientific literature, an interferometric fibre-optic sensor is described as a device that changes an optical wave phase change into an electrical signal. Optical fibre sensor can be applied to detect a wide variety of external signals. The influence of mechanical (vibration, acoustic wave, pressure, displacement), magnetic, electric fields or temperature on the lightwave propagation can be easily detected even in a closed optic circuit [1]. Optic fibre interference sensors have extremely high sensitivity and closed optic circuit that is their another advantage.

The fibre optic sensor consists of light source, optic fibre, and light detector which gives electric output signal. Optical fibre circuit has a sensing element – phase converter that changes the phase of lightwave according to external signal. Those changes are converted back to electric signal in a detector being an integral part of a demodulator unit.

Main advantage of fibre interferometers is possibility of measurement of phase changes of interference light beams, similarly as using typical interferometers, i.e., within the range of 10^{-6} radians while the light is guided in the closed optical loop. The measured value, which is implicit function, can be retrieved as an explicit function by means of optoelectronic demodulation systems.

Fibre optic interferometers are widely used in measurements where, as a rule, amplitude of non-modulated optical wave with optical frequency approximately THz is used [2].

2. Interferometric analysis of a distributed sensor

Single mode fibre optic carries coherent light wave of the properties similar to a plane wave and is capable to interfere. A distributed fibre optic sensor in Michelson interferometer layout is presented in Fig. 1.

The phase perturbation along the path L_1 can be obtained on the basis of interference of waves reflected from both arms of a sensor. Additional phase shift is introduced to achieve a clear distinction between consecutive wave packets.

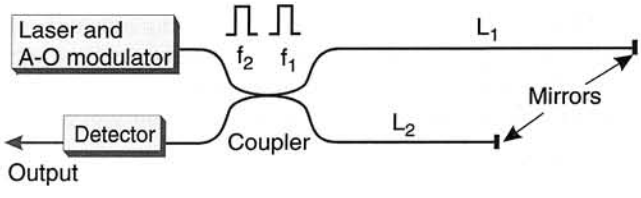

Fig. 1. Unbalanced Michelson's interferometer as a distributed sensor.

*e-mail: mchojnacki@wel.wat.waw.pl

If both arms of this interferometer are equal, it is called the balanced interferometer. If the lengths of interferometer arms are different (that is $L_1 \neq L_2$) it is called the unbalanced one. A Bragg cell (Fig. 2) works as a light frequency shifter [3].

The interferometer is excited with wave packets shorter than their propagation time through the arm. The delay between packets is set to obtain interference in the coupler

$$\tau = \frac{2L}{v}, \tag{1}$$

where $L = L_1 - L_2$ is the difference of lengths of interferometer arms, v is the speed of light in optic fibre.

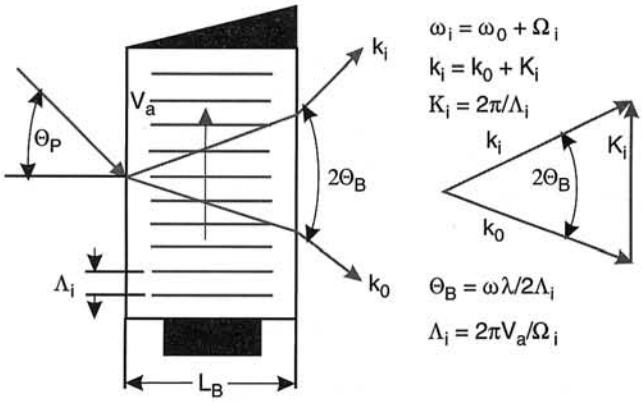

Fig. 2. Description of light frequency modulation with acoustooptic effect.

As a result, a signal proportional to a phase difference is obtained, having $\Delta f = f_1 - f_2$ frequency. A light wave at the output of frequency shifter (Fig. 2) with wave vector $\vec{k}_i = \vec{k}_0 + \vec{K}_i$ and the frequency $\omega_1 = \omega_0 + \Omega_1$ can be described as

$$E = \frac{1}{2} U_B e^{j(\Phi + \omega_1 t - \vec{k}_i \vec{r})}, \tag{2}$$

where U_B is the amplitude at the output of Bragg cell given by

$$U_B = U_p \sin\frac{\xi}{2}, \tag{3}$$

where U_p is the amplitude of incident wave, ξ is the Bragg angle.

To simplify this description, the following assumptions were made: optic coupling Bragg cell-fibre is lossless, the wave is divided with 1:2 ratio and the wave returning to the coupler after passing through the measurement arm can be described as

$$E_1 = \frac{1}{4} t_{m1} r_1 U_B e^{j(\Phi_1 + \omega_1 t - \beta L_1 + \delta_1)}, \tag{4}$$

where t_{m1} is the transmission coefficient, r_1 is the reflection coefficient, $\Phi_1 = \Phi + \Phi_z$ is the sum of initial phase and phase perturbation, δ_1 is the reflection-related phase change, and β is the propagation constant given by

$$\beta = n_1(\vec{k}_0 + \vec{K})(1 - \Delta_1 B), \tag{5}$$

where

$$\Delta_1 = \frac{n_1 - n_2}{n_1},$$

$$B = \frac{n_1^2 k_0^2 - \beta^2}{n_1^2 k_0^2 - n_2^2 k_0^2} = \frac{n_1^2 - n_{ef}^2}{n_1^2 - n_2^2}, \tag{6}$$

$$n_{ef} = \frac{\beta}{k_0}$$

Second wave packet reaches the coupler with the delay Δt ($t_2 = t - \Delta t$)

$$E_2 = \frac{1}{4} t_{m2} r_2 U_B e^{j(\Phi_2 + \omega_2 t_2 - \beta L_2 + \delta_2)}. \tag{7}$$

A light intensity can be expressed as

$$I = I_1 + I_2 + 2\sqrt{I_1 I_2}\cos\delta, \tag{8}$$

where

$$I_1 = \left(\frac{t_{m1} r_1 U_B}{4}\right)^2, I_2 = \left(\frac{t_{m2} r_2 U_B}{4}\right)^2, \tag{9}$$

$$\delta = \Phi_1 - \Phi + \omega_1 t - \omega_2 t_2 - \beta_1 L_1 + \beta_2 L_2 + \delta_1 - \delta_2. \tag{10}$$

Because

$$\begin{aligned} &\omega_i = \omega_0 + \Omega_i, \\ &\beta_i = n_1(\vec{k}_0 + \vec{K}_i)(1 - \Delta_i B), \\ &L_1 - L_2 = L \end{aligned} \tag{11}$$

which can be further rearranged into

$$I = I_1 + I_2 + 2\sqrt{I_1 I_2}\cos[\Phi_z(t) + \Delta\Omega t + \phi_d]. \tag{12}$$

The phase ϕ_d is a constant value resulting from constructional parameters of the interferometer ($k_o n_1 \Delta_1 BL$), environmental influences on arms of the interferometer, $\Delta\Omega = \Delta\Omega - \Omega_1$ difference of acoustic frequency, $\Phi_z(t)$ is the function of disturbance affecting measurement arm.

Equation (12) is called the transfer function of interferometer. It includes the required function of disturbance $\Phi_z(t)$. Introducing the parameter V, representing the interference contrast, the transfer function of interferometer can be described as

$$I(L) = P(1 + V\cos\delta), \tag{13}$$

where $V = \frac{|C|}{P}$, $\delta = \Delta\Omega t + \phi_d + \Phi_z(t)$,

$$P = \left(\sin\frac{\xi}{2}\right)^2 \left[\left(\frac{t_{m1}r_1}{4}\right)^2 + \left(\frac{t_{m2}r_2}{4}\right)^2\right] \int i_1(\vec{k}_0 + x)dx, \quad (14)$$

$$C(L) = 2\left(\sin\frac{\xi}{2}\right)^2 \frac{t_{m1}r_1}{4}\frac{t_{m2}r_2}{4} \times \times \int i_1(\vec{k}_0 + x)\cos(n_1 x \Delta_1 BL)dx, \quad (15)$$

$$S(L) = 2\left(\sin\frac{\xi}{2}\right)^2 \frac{t_{m1}r_1}{4}\frac{t_{m2}r_2}{4} \times \times \int i_1(\vec{k}_0 + x)\sin(n_1 x \Delta_1 BL)dx, \quad (16)$$

and $i_i(\vec{k}_0 + x)$ is the radiation spectrum of semiconductor laser.

The balance of the arms length of the interferometer considerably influences on detection ability of interferometer. If both arms of this interferometer are equal ($L = 0$), the interference contrast V can be written as

$$V = \frac{2\frac{t_{m1}r_1}{4}\frac{t_{m2}r_2}{4}}{\left(\frac{t_{m1}r_1}{4}\right)^2 + \left(\frac{t_{m2}r_2}{4}\right)^2} = D, \quad (17)$$

and depends only on transmission and reflection parameters of the interferometer. If these parameters in both arms of the interferometer are equal, the interference contrast is constant and equals nearly 1, ($V \approx 1$). For the unbalanced interferometer ($L \neq 0$), the interference contrast is always lower than 1 ($V < 1$).

A spectral distribution of the laser described by the following equation was use the interference contrast function of the interferometer for analysing

$$i_1(\vec{k}_0 + x) = i_0\left[\frac{e^{-(\alpha x+\beta)^2}}{2} + e^{-\alpha^2 x^2} + \frac{e^{-(\alpha x-\beta)^2}}{2}\right], \quad (18)$$

where α is the constant value depending on the half width of spectral line $\Delta\lambda$, β is the constant value linearly depending on a distance between the spectral main line and the spectral side lines.

This distribution is approximation of radiation spectrum of the semiconductor laser NDL 5030P made by NEC.

Course of interference contrast function was acquired from Eq. (13)

$$V(L) = D\exp\left[-\left(\frac{n_1\Delta_1 BL}{2\alpha}\right)^2\right]\frac{1+\cos\left(n_1\Delta_1 BL\frac{\beta}{\alpha}\right)}{2}. \quad (19)$$

where D is the constant given by Eq. (17).

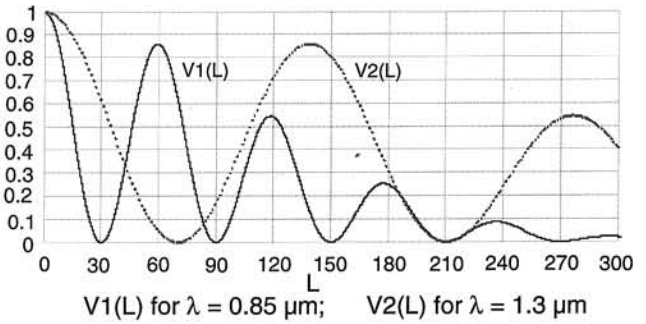

Fig. 3. Interference contrast change as a function of difference in length arms of the interferometer L.

Figure 3 illustrates influence of the wavelength change of the radiation source on the course of interference contrast function of the interferometer. The analysis was presented for two wavelengths λ with the same half width of the spectral line $\Delta\lambda$.

The function of the interference contrast has oscillatory character. It takes shape of fade sinusoid with the period and fading rate depending on the laser spectral characteristics. Increase in wavelength of radiation source improves the value of interference contrast, enlarges oscillation period, and reduces the fading rate.

As one can see, the function of interference contrast can assume a value equal to zero for small differences of the interferometer arms length L. Small changes of L, in the given range, can cause considerable changes of the interference contrast value V. A threshold of the interference contrast value is the sensitivity threshold of a photodetector.

3. Demodulation with application of the coupler 3×3

Optical fibre interferometer produces a high resolution optical output, but without an appropriate demodulation scheme, the output suffers from signal fading due to the changes in amplitude of the detected signal [4]. Many demodulation techniques have been developed to solve the signal-fading problem by using either a heterodyne or homodyne approach. Generally, heterodyne and homodyne demodulation schemes have good noise rejection and similar resolution. Heterodyne demodulations have better signal-to-noise ratio, however, its frequency modulator injects additional phase noise which corrupts the signal at low frequencies. On the other hand, active homodyne demodulations work well at low frequencies, but calibration or reset is required for its operation.

Recently, Jin *et al.* [5] have presented an algorithm to recover the change in phase from intensity outputs of either a quadrature or symmetric 3×3 coupler. Other demodulation techniques have been developed by Dandridge *et al.* [4], Bush and Sherman [6], and Brown *et al.* [7].

In demodulation, which uses fibre optic coupler 3×3, the input signals in the demodulator (Fig. 4) can be easily achieved from two outputs of the fibre optic coupler. In

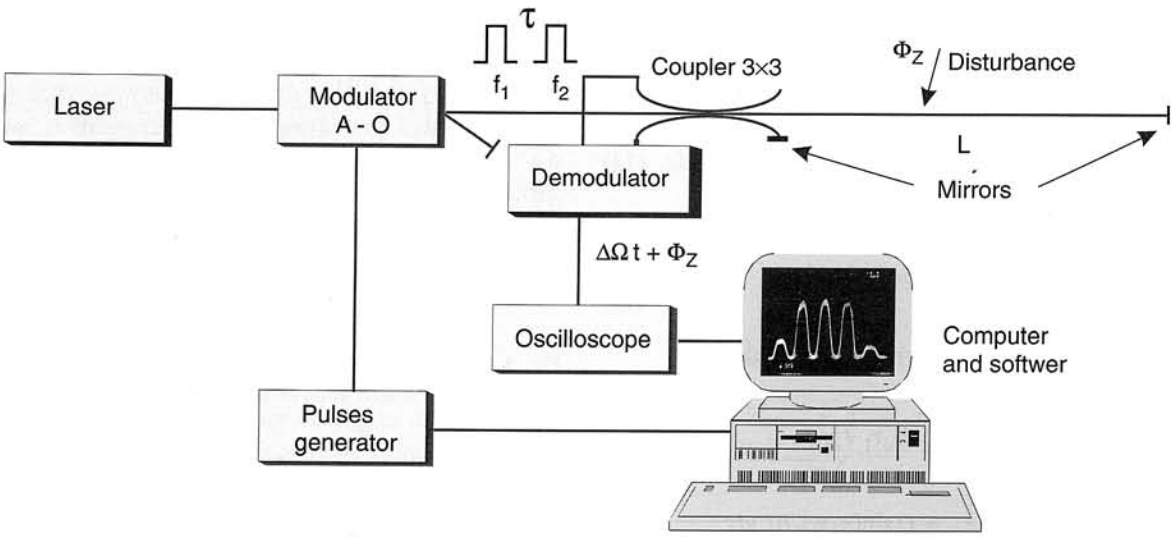

Fig. 4. Demodulation with the fibre optic 3×3 coupler.

that case, the fact that the output from 3-arm coupler contains the components which depend on $\cos\Theta(t)$ and $\sin\Theta(t)$, where $\Theta(t) = \Delta\Theta t + \phi_d + \Phi_z(t)$, $\phi_d = \bar{k}_0 n_1 \Delta_1 BL$ [7]. Thus,

$$\begin{aligned} I_1 &= -2B_2[1+\cos\Theta(t)], \\ I_2 &= B_1 + B_2\cos\Theta(t) + B_3\sin\Theta(t), \\ I_3 &= B_1 + B_2\cos\Theta(t) - B_3\sin\Theta(t), \end{aligned} \tag{20}$$

where B_1, B_2, and B_3 are the coefficients which depend on coupling coefficient in the coupler.

The signal with required phase shift $\pi/2$ can be achieved by the following operation

$$\begin{aligned} I_C &= I_2 + I_3 = 2B_1 + 2B_2\cos\Theta(t) \\ I_S &= I_2 - I_3 = 2B_3\sin\Theta(t) \end{aligned}. \tag{21}$$

The above signals, besides the coefficients depending on the coupler B_2, B_3, have an acceptable form for further processing. The output signal processing is known as a "differential-integral processing" and its block diagram is shown in Fig. 5. After differentiation, the output signals I_3 and I_2 are multiplied by the signals directly from photodetectors. Summing up these multiplied signals in a differential amplifier we can achieve the output as follows

$$I_S\frac{dI_C}{dt} - I_C\frac{dI_S}{dt} = \frac{d}{dt}[\Theta(t)]. \tag{22}$$

After the integration we achieve a signal which is mixed (Fig. 5) with a signal with differential frequency ($\Delta\Omega$). It gives, that the output signal linearly depends on the possible signal of disturbance $\Phi_Z(t)$ which influences on the measurement arm L

$$s_0 \approx \phi_d + \Phi_z(t). \tag{23}$$

This signal is a real function of the disturbance and can be separated from the drift ϕ_d by filtration. As availability of new high-speed digital processing (DSP) chips and high speed, high-resolution analogue-to-digital (A/D) converters improves, digital implementation of demodulation schemes becomes more feasible. By using the digital proceeding, noise (i.e. gain error and output drift) from analogue systems is reduced and better performance is expected. Taking advantage of the digital processing we built a microprocessor system that can carry out all demodulation operations in real time (Fig. 5).

The disturbance function, obtained in this way, can be used in the next steps of the signal processing:

- identification of kind of disturbance (animals, persons, vehicles) by means of reading model signals into a register of schemes and its comparison with current signals. As a degree of identification correctness a correlation coefficient higher then 0.95 can be used,
- localisation of the disturbance position for the sensor line divided into several sections.

In Fig. 5, we can distinguish the following steps:

- recording of signals from both interferometric channels,
- carrying out a spectrum analysis before demodulation,
- carrying out a process of differentiation and cross multiplication,
- showing the output function (the disturbance function with its spectrum analysis).

4. Conclusions

Fibre optic sensors with distributed sensitivity are still in progress. However, a few of them have been successfully applied and they are in use, i.e., OTDR in telecommunications and circuit sensors in security systems.

The above-presented sensor can be used in fibre optic security system for detection of invasion and to monitor telecommunication and energetic cables or gas mains. This sensor can be installed underground and assured the high-

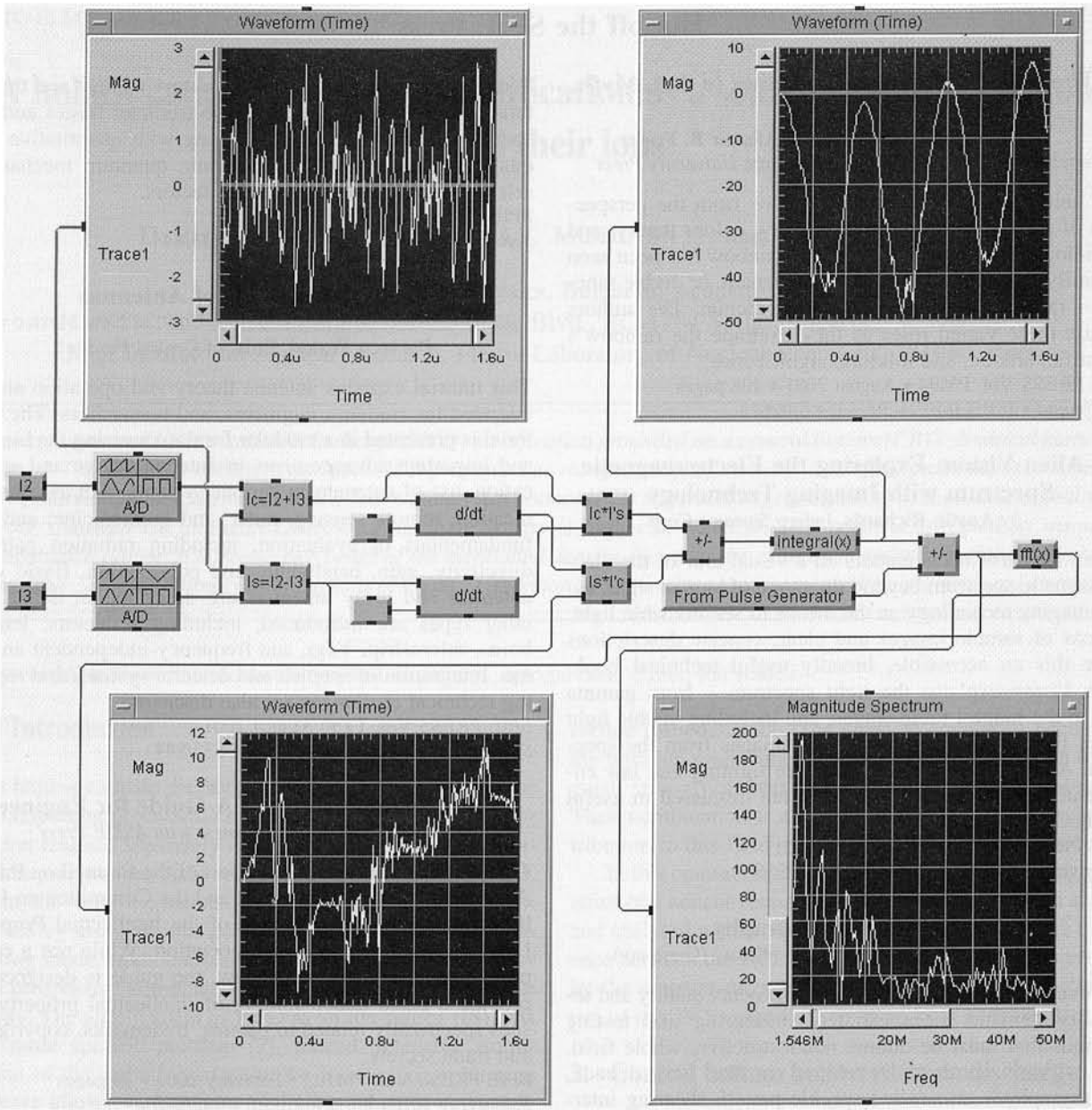

Fig. 5. Schematic diagram of digital demodulation with "differential – integral processing".

est level of security, because fibre optic is inherently undetectable and it does not emit any radiation.

Designing a fibre optic sensor one should analyse and choose the source of radiation λ and a difference in the interferometer arms L. Those parameters ensure high value of contrast what next assures better registration of perturbation and decrease in the number of false alarms.

References

1. M. Szustakowski and W.M. Ciurapiński, "Fibre optic distributed sensor", *Proc. SPIE* **3054**, 381–389 (1997).
2. M. Szustakowski, W.M. Ciurapiński, and L. Jodłowski, "Some issues on phase analysis", *Molecular and Quantum Acoustics* **20**, 263–277 (1999).
3. V.N. Mahajan, "Theory of acoustooptic interaction standing and travelling sound waves", *Wave Electronics* **2**, 309–339 (1976).
4. A. Dandridge, "Fibre optic sensor based on the Mach-Zehnder and Michelson interferometers", in *Fibre Optic Sensors: An Introduction for Engineers and Scientists*, pp. 271–323, edited by E. Udd, John Wiley&Sons, 1991.
5. W. Jin, D. Walsh, D. Uttamchandani, and B. Culshaw: "A digital technique for passive demodulation in a fibre optic homodyne interferometer", *The 1st European Conference on Smart Structures and Materials*, 57–60 (1992).
6. I.J. Bush and D.R. Sherman, "High performance interferometric demodulation techniques", *Proc. SPIE* **1795**, 412–420 (1992).
7. B. Chiu and M.C. Hastings, "Digital demodulation for passive homodyne optical fibre interferometry based on a 3×3 coupler", *Proc. SPIE* **2292**, 371–381 (1994).